



Contents lists available at ScienceDirect

International Journal of Thermal Sciences

journal homepage: www.elsevier.com/locate/ijts

Unsteady natural convection cooling of a water storage tank with an internal gas flue

I. Hmouda^{a,*}, I. Rodriguez^b, C. Bouden^a, A. Oliva^b

Q1

^a Research Group: Energy in Buildings and Solar Energy, National School of Engineers of Tunis, BP 37, Le Belvédère 1002 Tunis, Tunisia^b Heat and Mass Transfer Technological Centre (CTTC), Polytechnical University of Catalonia (UPC), Colom 11 08222, Terrassa, Barcelona, Spain

ARTICLE INFO

Article history:

Received 5 November 2008

Received in revised form

14 April 2009

Accepted 26 May 2009

Available online xxx

Keywords:

Natural convection

CFD simulations

Experimental set-up

Storage tanks

Model development

ABSTRACT

The cooling process by natural convection in cylindrical cavities is a phenomenon which takes place in several applications such as solar energy systems. In the present work a storage tank with an internal gas flue is studied experimentally and numerically during its long-term cooling process. The computational domain includes two fluids, i.e. water in the store and air in the chimney, and two external and internal layers of steel separated by polyurethane insulation material. In this paper, the numerical and the experimental analysis of the temperature field inside the tank submitted to an external convection cooling process with a constant convection heat transfer coefficient is presented. The air and the water temperature profiles along the vertical lines are obtained experimentally and numerically, for a cooling period of 90 h. The numerical analysis is carried out using a specific CFD code developed for the present work; an axisymmetric domain has been considered. Finally, a detailed description of the phenomena that occur inside the water part of the domain during the cooling process is also provided.

© 2009 Published by Elsevier Masson SAS.

1. Introduction

A cylindrical tank of liquid water with a gas chimney which is crossing the tank from the bottom to the top is one of the practical configurations that has been widely used as a heating system. In order to enhance the thermal efficiency of such system, its configuration should be optimised. This effective optimisation requires an extensive knowledge of the thermal and fluid dynamic behaviour of the fluid in the tank, and its relationship with the air inside the gas flue and with the tank walls and thermal insulation.

However, on some situations, designs are based in simple mathematical models (e.g. one-dimensional models), that together with expensive trial-and-error experimental set-ups provide the empirical parameters necessary for those models. The main advantages of the one-dimensional models are their simple implementation and their reduced CPU time when long-term simulations are carried out. This kind of models is often used in commercial global codes such as TRNSYS [1]. In these models, the tank is modelled by means of energy balance in a fixed number of fluid volumes and the temperature of each volume is considered uniform [2,3]. Comparisons and results analysis of simulations performed using these models can be found in [2,4,5]. When a new

element (such as a gas flue inside the tank) is introduced in the system, the one-dimensional model becomes inadequate. Thus, empirical parameters have to be introduced in order to model the global system.

In this sense, in the last decades, detailed numerical simulations of heat transfer and fluid flow using Computational Fluid Dynamics (CFD) codes have become a powerful tool for studying the complex phenomena taking place in these equipment. Several works describing the unsteady cooling or heating processes of a fluid inside an enclosure can be found in the literature. Among these studies, the work conducted by Hyun [6] can be cited. He studied the transient process of stratification of a fluid in a closed cylinder initially at rest, by imposing a temperature gradient in its lateral wall. His work provided earlier evidence of the mechanism of stratification and the influence of buoyancy forces in the circulation of the fluid. Cotter and Charles [7,8] investigated the transient cooling process of warm crude oil confined in a vertical cylinder. In the study, the influence in the heat losses of the aspect ratio, external heat loss coefficient, as well as the fluid viscosity were analysed. Furthermore, the numerical results were compared with experimental data and a time dependence correlation of Nusselt number for several oil viscosities was defined.

Papanicolaou and Belessiotis [9] studied numerically the natural convection in a vertical cylindrical enclosure heated from the sidewall with constant heat flux and at high Rayleigh numbers. From a numerical point of view, a good agreement between the

* Corresponding author. Tel.: +216 71 874 700; fax: +216 71 872 729.

E-mail address: imen.hmouda@enit.rnu.tn (I. Hmouda).

Nomenclature

c_p	specific heat at constant pressure ($\text{J kg}^{-1} \text{K}^{-1}$)
n_{ins}	number of control volumes in insulation
D	tank diameter (m)
n_e	number of control volumes in external wall
D_c	chimney diameter (m)
\overline{Nu}	average Nusselt number
\vec{g}	acceleration of gravity vector (m s^{-2})
p_d	dynamic pressure (Pa)
H	tank height (m)
Pr	Prandtl number
H_c	water store height (m)
S	inner area of the tank (m^2)
h_{ext}	external superficial heat transfer coefficient ($\text{W m}^{-2} \text{K}^{-1}$)
t	time (s)
k	thermal conductivity ($\text{W m}^{-1} \text{K}^{-1}$)
Δt	time increment (s)
k_e	thermal conductivity of the external solid wall ($\text{W m}^{-1} \text{K}^{-1}$)
\bar{T}_f	mean fluid temperature (K)
q''	heat flux per unit surface area (W/m^2)
\bar{T}_w	mean inner wall temperature (K)
Ra	Rayleigh number
T	temperature (K)

r	radial coordinate (m)
T_{ini}	initial temperature (K)
n_r	number of control volumes in radial direction
T_{amb}	ambient temperature (K)
n_z	number of control volumes in axial direction
T_{ref}	reference temperature $T_{\text{ref}} = (T_{\text{ini}} + T_{\text{amb}})/2$ (K)
n_c	number of control volumes in chimney
v_r	radial velocity (m s^{-1})
n_s	number of control volumes in internal solid wall
v_z	axial velocity (m s^{-1})
n_w	number of control volumes in water part
\vec{v}	velocity vector (m s^{-1})
z	z-coordinate (m)

Greek letters

α	thermal diffusivity ($\text{m}^2 \text{s}^{-1}$)
δ_{ins}	insulation thickness (m)
β	thermal expansion (K^{-1})
δ_{in}	internal wall thickness (m)
ρ	density (kg m^{-3})
δ_{ex}	external wall thickness (m)
μ	dynamic viscosity (Pa s)
$\vec{\tau}$	stress tensor vector (kg m s^{-2})
Ω	water volume (m^3)
ϵ	relative error (%)
θ	non-dimensional temperature

model predictions and the experimental data for both the laminar and the turbulent regimes was found. Moreover, one of the goals of their work was to study the performance of several turbulence models for their use in the unsteady simulation of cylindrical configurations, shedding some light about the fluid regime present in real working conditions.

Lin and Armfield [10] studied numerically the cooling process of an initially homogeneous fluid in a vertical cylindrical tank by natural convection. In their work, the top and the bottom walls were maintained adiabatic while the lateral wall was suddenly cooled. In a later paper, the same authors [11] analysed the long-term behaviour of cooling a fluid in a cylindrical tank considering two different situations: one with an imposed sidewall temperature and the other with fixed side and bottom wall temperatures while the other walls were maintained adiabatic. Using the numerical results, scaling relations for the mean fluid temperature and Nusselt number have been obtained for each situation. Although their study was in non-dimensional form, because of the imposed boundary conditions, the correlations they found can not be extended to the real situation of a cylindrical tank submitted to the unsteady natural convection due to heat losses to the environment.

The cooling process of a real prototype of storage tank was studied numerically and experimentally by Oliveski et al. [12]. They analysed the transient phenomena taking place due to the heat exchange with the environment. In their work, the influence of the aspect ratio, the volume and the insulation thickness on the thermal performance of the tank was studied. A good agreement between the numerical and experimental results was observed. Furthermore, a correlation for the Nusselt number for each tank volume, function of the previously mentioned parameters, was developed. Adopting the same methodology, the same authors [13], compared the results of a one-dimensional model with those obtained from a detailed model and to the experimental results. They have shown that the simplified model agreed with the

experimental results only when several computational artifices were included.

Fernandez-Seara et al. [14], carried out an experimental analysis of the thermal performance of a commercial hot water storage tank under the static mode of operation. The main purpose of their work was to determine the thermal behaviour of the tank in order to characterise its performance, while at the same time determining its overall heat transfer coefficient. For the analysis, they used the experimental results for quantifying the degree of thermal stratification and the exergy efficiency.

More recently, Rodríguez et al. [15] carried out a scaling analysis and numerical simulation of the transient process of cooling-down of an initially homogeneous fluid in a vertical cylinder submitted to natural convection. The correlations obtained can be extrapolated to other situations as they are expressed in term of non-dimensional parameters governing the phenomena that occur inside the tank.

All the mentioned numerical and experimental studies have been carried out in standard cylindrical tanks. However, the results obtained in the aforementioned works can not be extrapolated to the configuration under study in the present paper, i.e. a water storage tank with an internal gas flue. As far as the author's knowledge is concerned, there are no previous works in the literature modelling in detail this configuration of storage tank. In fact, this configuration has only been studied by means of one-dimensional models [16–19]. In these works, the fluid inside the tank and the air inside the gas flue were modelled by means of a multinode approach. For the coupling of both media, the values of the superficial heat transfer coefficients must be supposed. Furthermore, obtaining realistic results required the inclusion of computational artifices (e.g. procedures that examine for each time step the distribution of the temperatures and, in the case of finding hotter water layers under colder ones, artificially mix or interchange the layers of water). Under these circumstances, these models are not capable of describing in detail the transient

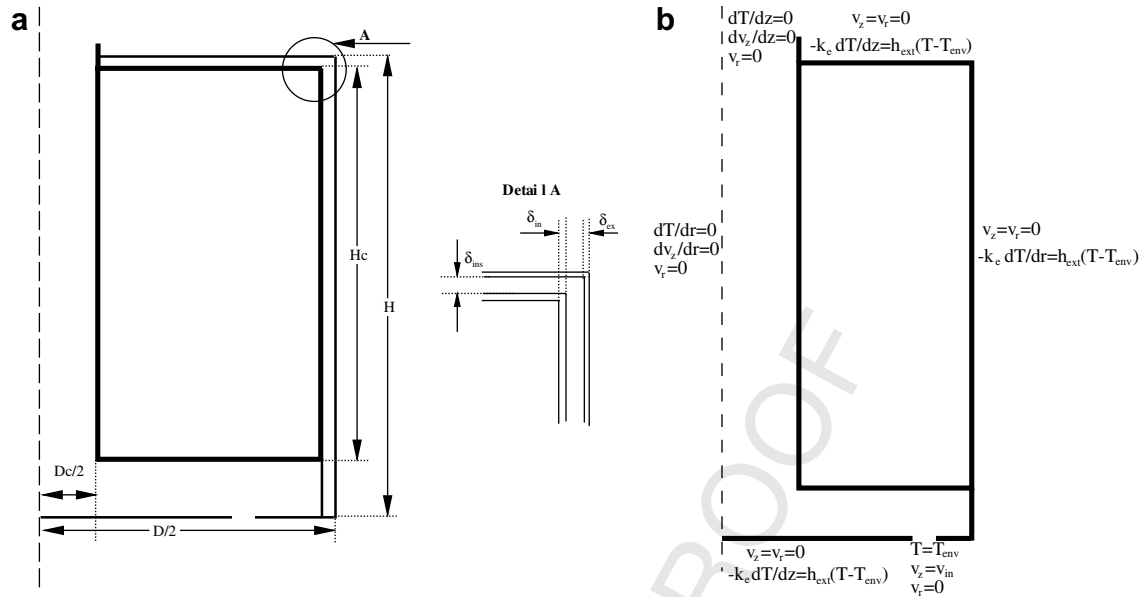


Fig. 1. a) Schematic of the geometry and b) the boundary conditions of the storage tank under study.

temperature profile of the stored fluid. In [18] the large differences between experimental data and simplified models were shown. These results prove the need of implementing detailed numerical models for studying the thermal and fluid dynamic behaviour of the fluid inside the tank.

The case is not only of fundamental interest to fluid mechanics and heat transfer, but also of importance in many practical applications. In fact, the studied tank configuration corresponds to a large number of domestic gas boilers. Studying this system will

contribute to understand the cooling process due to unsteady natural convection in this model of boilers.

The aim of this paper is to investigate numerically and experimentally, the unsteady natural convection of a vertical cylindrical storage tank with an internal gas flue submitted to heat transfer to the environment. The numerical solution has been obtained using a developed CFD code which has been submitted to a verification process by considering different bench-mark cases found in the literature. After the validation of the code with comparison to the

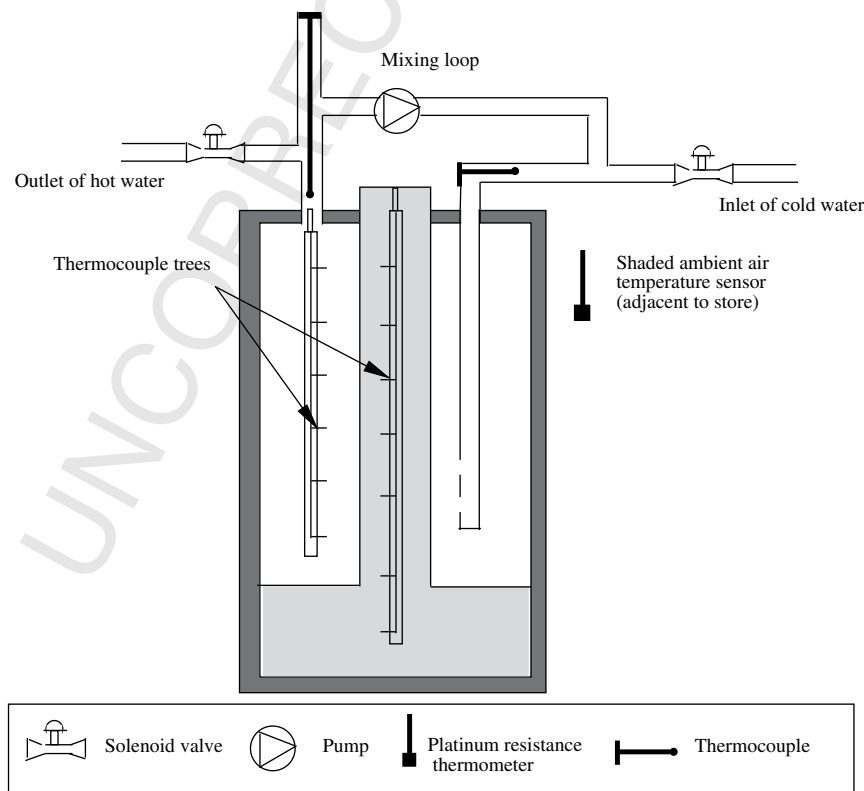


Fig. 2. The experimental set-up of the storage tank.

Table 1
Thermo-physical properties used in the simulation.

Property	Material			
	Water	Air	Steel	Insulation
ρ [kg/m ³]	996.2	1.16	8030	70
c_p [J/kg K]	4164.4	1007	502	1045
k [W/m K]	0.615	0.0263	15.27	0.06
μ [Pa s]	8.07×10^{-4}	1.8×10^{-4}	–	–
β [1/K]	2.76×10^{-4}	3.3×10^{-3}	–	–

Table 2
Number of CVs in the h-refinement including the fluids and solid walls
 $n_r \times n_z = (n_c + n_s + n_w + n_{ins} + n_e) \times (n_e + n_c + n_s + n_w + n_{ins} + n_e)$.

	$n_r \times n_z$	Mesh distribution
m_1	20×40	$(4 + 1 + 12 + 1 + 1 + 1) \times (1 + 8 + 1 + 31 + 1 + 1 + 1)$
m_2	30×64	$(6 + 1 + 19 + 1 + 2 + 1) \times (1 + 12 + 1 + 46 + 1 + 2 + 1)$
m_3	44×95	$(8 + 2 + 28 + 2 + 3 + 1) \times (1 + 18 + 2 + 68 + 2 + 3 + 1)$
m_4	65×141	$(12 + 3 + 42 + 3 + 4 + 1) \times (1 + 27 + 3 + 102 + 3 + 4 + 1)$

experimental results, the transient physical phenomena occurring in the storage tank has been also described in detail.

2. Experimental set-up

The experimental test has been performed in a vertical cylindrical tank with an internal gas flue. An schematic of the tank is shown in Fig. 1(a). The tank has a volume of water of $0.144m_3$ with an external aspect ratio of $H/D = 2.24$ ($H = 1.132$ m, $D = 0.505$ m). Composite tank walls are made of 3 mm steel (δ_{in}), 2 cm of polyurethane thermal insulation (δ_{ins}) and 1 mm of steel at the external part (δ_{ex}). A chimney with a diameter (D_c) about 0.1 m is crossing the tank from the bottom to the top ($H_c = 0.932$ m), which gives a supplementary heat exchange surface between the hot gas and the water in the tank. The chimney is connected to a combustion chamber located at the bottom part of the tank. In the bottom part of the combustion chamber, there is a ring which provides the entrance of the air necessary to the combustion.

The outlet and the inlet of the water have been inserted from the top of the tank. Cold water has been conducted to the bottom of the tank with a linear-slot diffuser (see Fig. 2).

The temperature measurements required for the storage tank analysis have been: the cold water temperature, inlet and outlet temperatures, the ambient temperature and the temperatures at different levels in the store, in the gas flue and in the combustion chamber. A tree of six thermocouples have been set inside the tank, at 15 cm distance from each other, for recording the temperature of the stratified layers. Five other thermocouples have been mounted in the centre of the chimney for measuring the air temperature. The experimental set-up is shown schematically in Fig. 2. Considering the different environments for temperature measurements (water,

air) and the required accuracies, diverse transducers have been chosen. According to the temperature range, the K-type (Chromel/Alumel) thermocouples have been used for the storage tank while a platinum resistance thermometer (PT100) has been used for ambient temperature measurement.

As the experimental data have been used in numerical results validation, it has been essential to carry out accurate temperature measurements. Thus, calibration of all temperature sensors has been performed. In all cases, it has been shown that the sensors accuracy have been less than 0.4°C .

To precondition the hot water inside the tank to a uniform temperature, a mixing loop has been used to circulate the fluid from the top to the bottom of the tank. When the temperature difference between the inlet and the outlet has been less than 1°C for a 15 min period, the tank has been left to cool-down for a 90 h period. During this cooling process, the temperature has been measured every 30 s for all the locations. The measured information has been recorded with data acquisition HP Benchlink Data Logger unit connected to a personal computer.

3. Mathematical and numerical models

This section describes the basic formulation and numerical approach used to solve the complex phenomena taking place inside the tank. The domain involves the two fluids (water inside the store and air inside the flue), an internal steel wall, and a polyurethane insulating material covered by a uniform thin layer of steel at external walls.

3.1. Governing equations

The fluid flow and heat transfer phenomena for the problem under study is governed by the Navier–Stokes and the energy conservation equations. In numerical simulations of real cases, such as the problem described in the previous section, it is important to determine if the flow regime can be assumed to be laminar or if a turbulence model has to be used. In fact, there is a lack of information in the literature, e.g. critical Rayleigh number, to be used as a reference in those cases. In such specific situations, detailed numerical experiments of the heat transfer and fluid dynamic phenomena taking place can be a means for solving and studying the fluid regime inside the tank. An example of such experiments are those conducted by [20] for a differentially heated air-filled cavity of aspect ratio 4. However, the Direct Numerical Simulation (DNS) of the long-term cooling process of the storage tank would require a large amount of computational resources and, together with the requirements for solving all the transient scales, could be cumbersome.

On the other hand, studies carried out in similar working conditions, can give some informations about fluid regime in such

Table 3
Average fluid temperature, wall temperature at the liquid–solid interface and Nusselt number. Comparison results between different levels of refinement for $t = 900$ –3600 s.

	$t = 900$ s						$t = 1800$ s					
	\bar{T}_f [°C]	$\epsilon \cdot 10^2$ [%]	\bar{T}_w [°C]	$\epsilon \cdot 10^2$ [%]	\bar{Nu} [–]	ϵ [%]	\bar{T}_f [°C]	$\epsilon \cdot 10^2$ [%]	\bar{T}_w [°C]	$\epsilon \cdot 10^2$ [%]	\bar{Nu} [–]	ϵ [%]
m_1	65.459	1.1	64.815	1.179	290.536	4.5	65.083	2.6	64.375	4.4	285.842	5.6
m_2	65.457	0.7	64.823	0.034	290.055	4.7	65.073	1.2	64.369	3.5	291.745	3.7
m_3	65.457	0.7	64.823	0.019	292.996	3.7	65.072	1.0	64.351	0.6	302.007	0.32
m_4	65.452	–	64.823	–	304.492	–	65.065	–	64.347	–	302.993	–
	$t = 2700$ s						$t = 3600$ s					
	\bar{T}_f [°C]	$\epsilon \cdot 10^2$ [%]	\bar{T}_w [°C]	$\epsilon \cdot 10^2$ [%]	\bar{Nu} [–]	ϵ [%]	\bar{T}_f [°C]	$\epsilon \cdot 10^2$ [%]	\bar{T}_w [°C]	$\epsilon \cdot 10^2$ [%]	\bar{Nu} [–]	ϵ [%]
m_1	65.083	2.6	64.376	4.4	285.843	5.6	64.688	4.3	63.951	5.2	283.638	1.8
m_2	65.074	1.2	64.370	3.5	291.745	3.7	64.677	2.7	63.952	5.4	285.206	1.3
m_3	65.072	1.0	64.351	0.6	302.008	0.3	64.678	2.8	63.917	0.1	292.366	1.1
m_4	65.066	–	64.347	–	302.994	–	64.659	–	63.917	–	289.118	–

Table 4

Cont. Average fluid temperature, wall temperature at the liquid–solid interface and Nusselt number. Comparison results between different levels of refinement for $t = 4500$ –7200 s.

	$t = 4500$ s						$t = 5400$ s					
	\bar{T}_f [°C]	$\epsilon \cdot 10^2$ [%]	\bar{T}_w [°C]	$\epsilon \cdot 10^2$ [%]	\bar{Nu} [–]	ϵ [%]	\bar{T}_f [°C]	$\epsilon \cdot 10^2$ [%]	\bar{T}_w [°C]	$\epsilon \cdot 10^2$ [%]	\bar{Nu} [–]	ϵ [%]
m_1	63.892	7.4	63.102	12.8	269.998	4.0	63.501	9.8	62.689	16.8	261.898	5.7
m_2	63.884	6.2	63.089	10.7	262.477	1.1	63.490	7.9	62.690	16.9	263.169	6.3
m_3	63.881	5.7	63.069	7.6	261.535	0.7	63.486	7.3	62.648	10.2	252.960	2.1
m_4	63.844	–	63.021	–	259.540	–	63.439	–	62.584	–	247.551	–
	$t = 6300$ s						$t = 7200$ s					
	\bar{T}_f [°C]	$\epsilon \cdot 10^2$ [%]	\bar{T}_w [°C]	$\epsilon \cdot 10^2$ [%]	\bar{Nu} [–]	ϵ [%]	\bar{T}_f [°C]	$\epsilon \cdot 10^2$ [%]	\bar{T}_w [°C]	$\epsilon \cdot 10^2$ [%]	\bar{Nu} [–]	ϵ [%]
m_1	63.120	13.2	62.278	19.3	250.785	2.8	62.762	19.9	61.899	25.0	246.098	5.3
m_2	63.098	9.7	62.272	18.4	252.711	3.6	62.710	11.6	61.866	19.5	246.756	5.5
m_3	63.093	8.9	62.234	12.3	244.386	0.2	62.704	10.6	61.827	13.2	237.399	1.5
m_4	63.037	–	62.157	–	243.774	–	62.637	–	61.745	–	233.672	–

situations. Among these studies, can be mentioned the work of Papanicolaou and Belessiotis [9], who investigated the transient heating of a fluid by an imposed heat flux at the sidewall for Rayleigh numbers between $10^{10} \leq Ra \leq 10^{15}$. In their study, they found that laminar regime can be obtained up to $Ra = 10^{13}$, while turbulent flow should be expected for $Ra > 5 \times 10^{13}$. Defining Rayleigh number as a function of the heat flux through the walls [21], $Ra = \rho g \beta q'' H_c / k \mu \alpha$; at the beginning of the cooling process the maximum value achieved is $Ra = 3.8 \times 10^{12}$. As the fluid is cooled down, heat losses to the environment decrease with the resulting decrease of the Rayleigh number. Considering this, in the present work the flow has been supposed laminar.

The following assumptions are considered: (i) the fluid is Newtonian, (ii) the thermo-physical properties are considered to be constant, (iii) the Boussinesq approximation is considered in the water domain: the water density is variable in the buoyancy terms of the momentum, (iv) viscous dissipation is negligible and (v) non-participant radiating medium is supposed. Thus, the governing equations can be written as follows:

$$\nabla \cdot \vec{v} = 0 \quad (1)$$

$$\frac{\partial \vec{v}}{\partial t} + \vec{v} \cdot \nabla \vec{v} = -\frac{1}{\rho} \nabla p_d + \frac{1}{\rho} \nabla \cdot \vec{\tau} - \vec{g} \beta (T - T_{ref}) \quad (2)$$

$$\frac{\partial T}{\partial t} + \vec{v} \cdot \nabla T = \alpha \nabla^2 T \quad (3)$$

3.2. Boundary and initial conditions

Considering the symmetry of the problem defined, the computational domain has been assumed to be axisymmetric. No-slip conditions have been used as boundary conditions for the momentum equations at all solid walls, while at the axis, symmetry boundary condition has been imposed. In the energy equation, every external tank wall (bottom, side and top) has been submitted to external convection actions, thus the overall convection heat transfer coefficient used has been set to $h_{ext} = 10 \text{ W/m}^2 \text{ K}$. This coefficient has been experimentally found in the laboratory [22]. In order to complete the thermal boundary condition, experimental records of environmental temperature have been used. As the measured environmental temperature has not been directly introduced into the model in each time step, the boundary condition for the simulation has been fixed at the average value of experimental records i.e. at 19°C .

The boundary conditions assumed at the inlet and the outlet of the gas flue are rather more complicated because the inappropriate formulation of these boundary conditions may lead to a large

difference between the model predicted fluid flow and heat transfer and the real case under study. The air has been assumed to enter at the combustion chamber from the surroundings with a temperature equal to ambient temperature and with an axial velocity equal to 0.01 m/s . This value has been estimated using experimental data measured at the outlet of the flue. However because in the experimental prototype, the combustion chamber has many orifices; it was very difficult to estimate the real mass flow rate of the entering air.

At the chimney outlet, the temperature gradient has been assumed null in the axial direction and all the kinematic energy of the air has been assumed to be converted to heat, resulting into an outlet dynamic pressure equal to the surrounding air dynamic pressure, i.e. equal to 0 ($\partial T / \partial n|_{outlet} = 0$ and $p_d|_{outlet} = 0$). An initial condition of uniform temperatures has been imposed for the whole domain. These temperatures have been fixed at 65°C for water and 50°C for the air, while velocities have been supposed to be null (see Fig. 1(b)).

3.3. Numerical approach

The numerical solution has been obtained over the whole domain by discretising the governing equations by means of finite

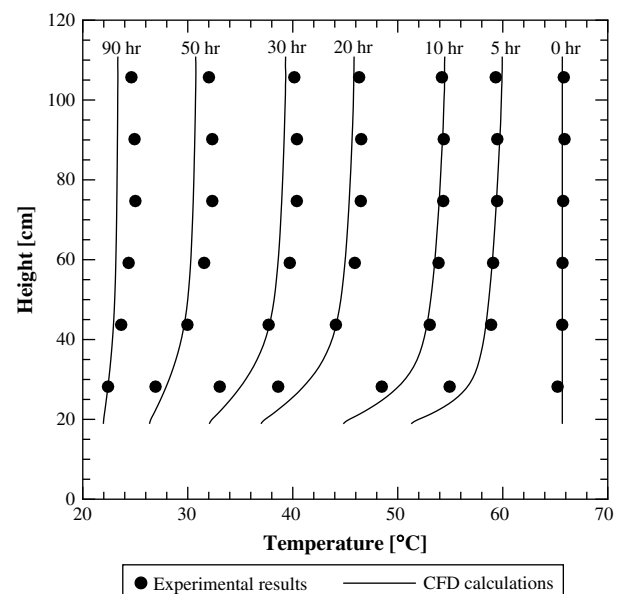


Fig. 3. Comparison between the temperatures obtained from the experimental set-up and from the numerical model for different instants of the cooling process.

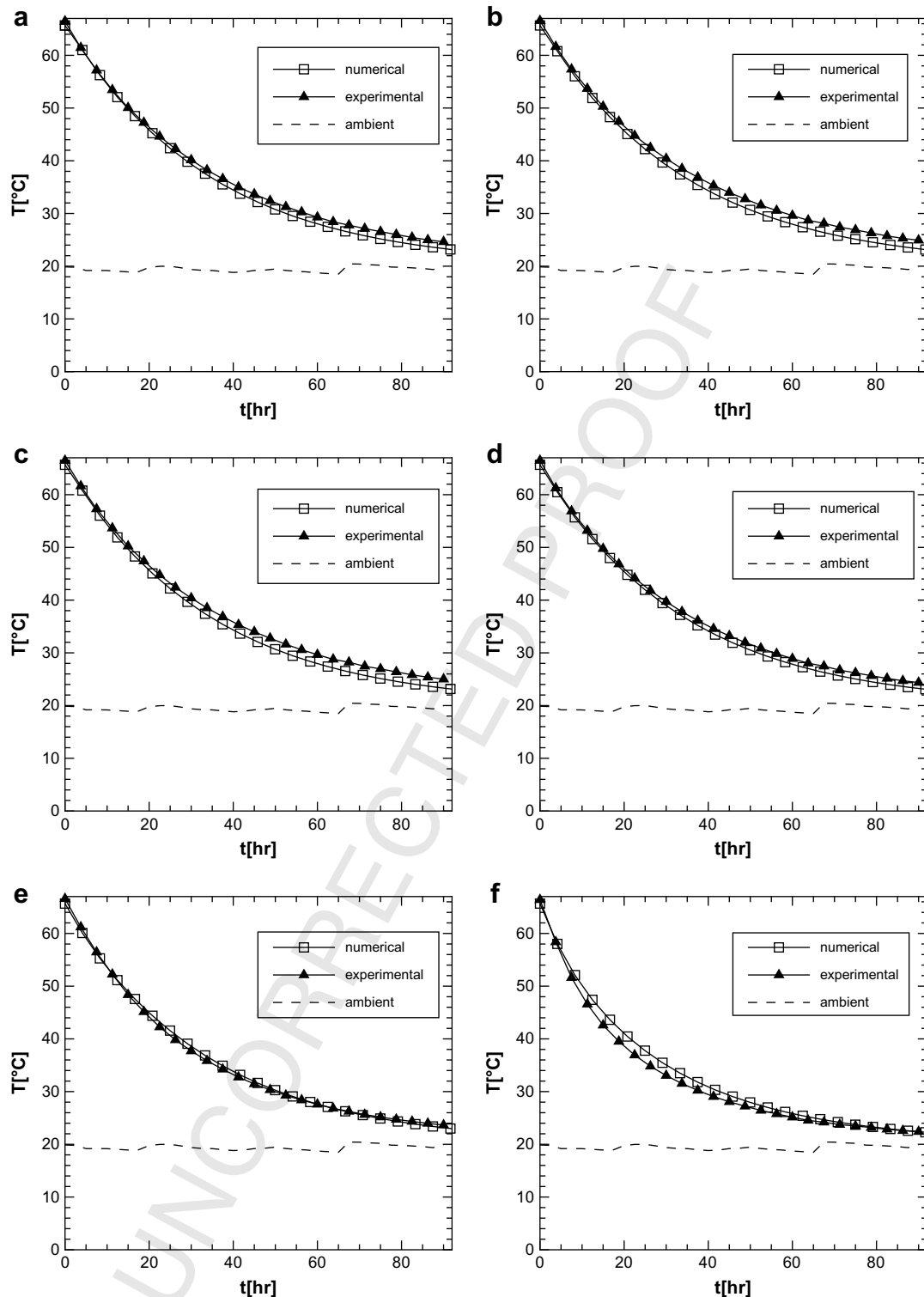


Fig. 4. Comparison of the water temperature obtained from the experimental set-up and from the numerical model for a 90 h of cooling process. (a) $z = 1.057$ m; (b) $z = 0.902$ m; (c) $z = 0.747$ m; (d) $z = 0.592$ m; (e) $z = 0.432$ m; (f) $z = 0.282$ m.

volume techniques as described by Patankar [23]. Fully implicit first order temporal differentiation using cylindrical grids on a staggered arrangement has been implemented. Diffusive terms have been evaluated using second order central differences scheme, while convective terms have been approximated by means of high order SMART scheme using a deferred correction approach [24]. The pressure-velocity coupling has been solved by using a SIMPLE-C

algorithm [25]. The resulting equation for pressure has been solved using the direct Band LU solver [26] while the algebraic system of linear equations for the velocities and temperature have been calculated using TDMA line by line solver [23].

In each time step, the fixed convergence criteria requires that the non-dimensional variables increments and residuals have been lower than 10^{-4} . The case has been solved during 90 h of the cooling process.

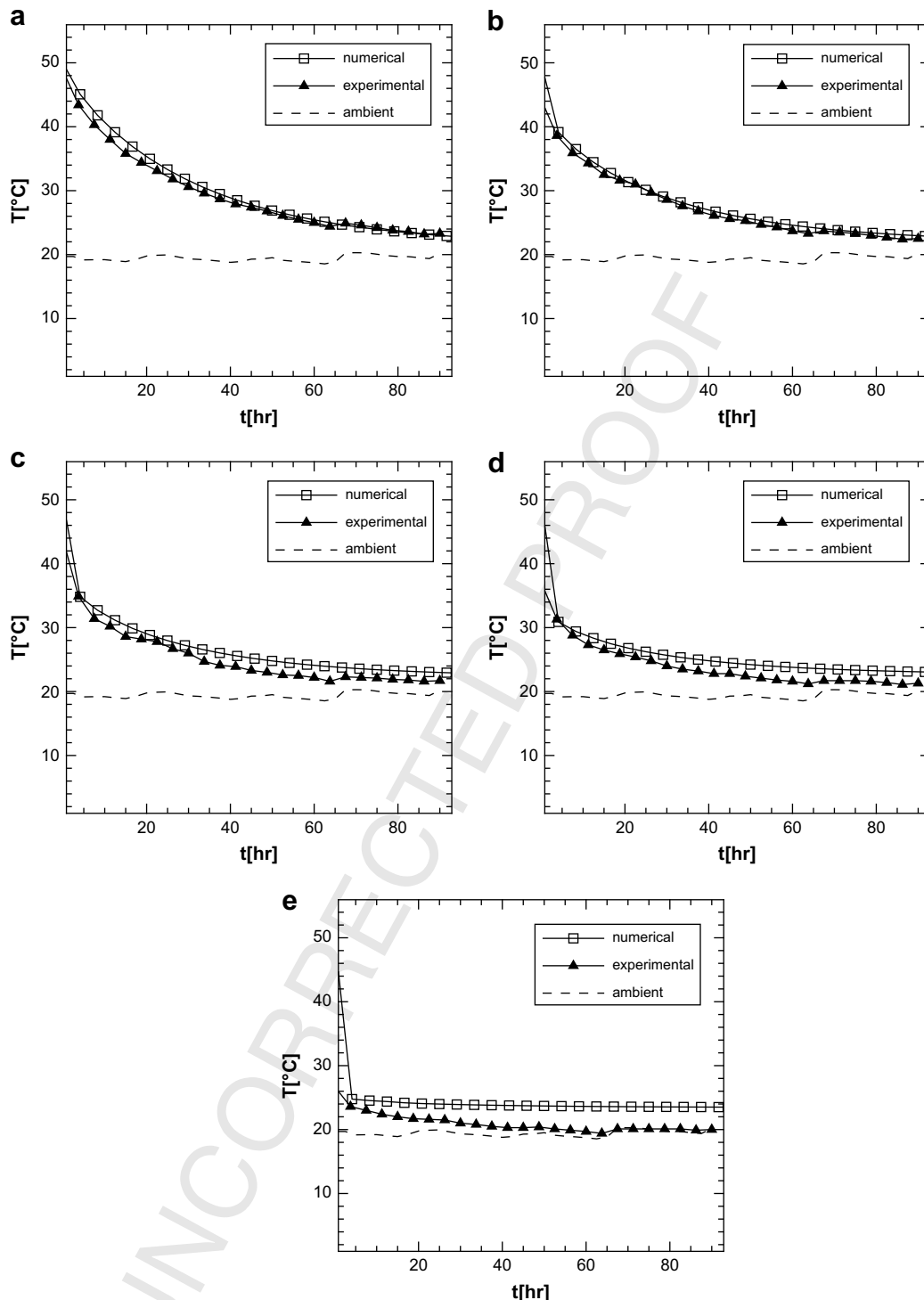


Fig. 5. Comparison of the air temperature obtained from the experimental set-up and from the numerical model for a 90 h of cooling process. (a) $z = 1.037$ m; (b) $z = 0.747$ m; (c) $z = 0.572$ m; (d) $z = 0.422$ m; (e) $z = 0.107$ m.

The thermo-physical properties used are listed in Table 1. As observed by Oliveski et al. [12] thermal gradients are the largest near the interface fluid/solid. Thus, the mesh has been concentrated in the regions near the walls, while uniform meshes have been used in the solid walls and the insulation materials. In the fluid domain, a tanh-like function with a concentration factor of 2, see [27], has been adopted in the radial and axial directions to properly solve the boundary layer.

4. Results

4.1. Numerical solution verification

The magnitude of the heat flux at the tank wall determines the degree of grid refinement needed to obtain a stable solution; the larger the thermal gradients found in boundary layer region is, the higher the number of control volumes needed. The numerical

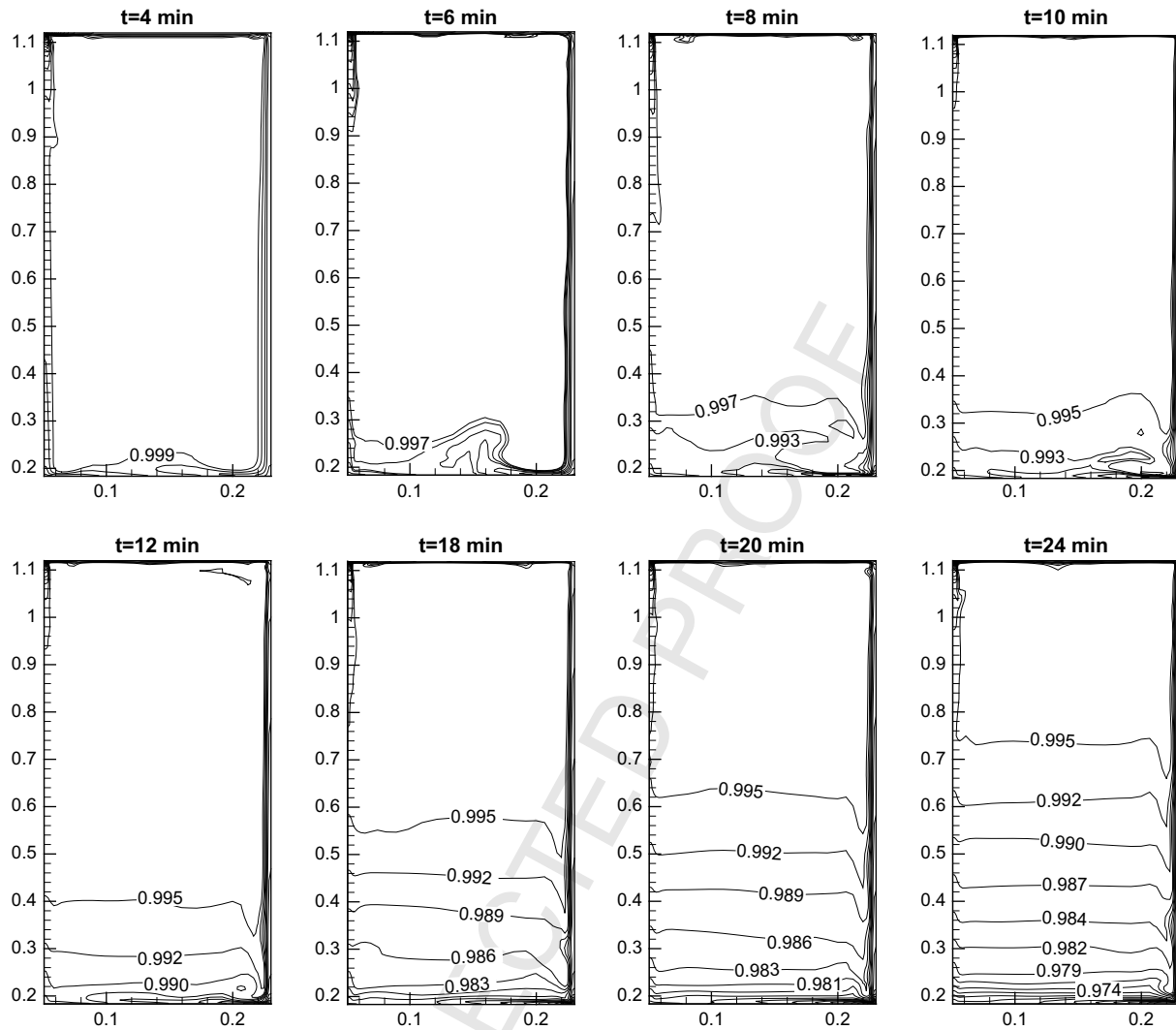


Fig. 6. Transient evolution of the fluid inside the water store. Dimensionless temperature contour during cooling process for time = 4–24 min.

solutions introduced in this work have been submitted to a process of verification adopting a h-refinement criteria. That is, fixing numerical schemes, the verification process accounts for the influence of the mesh spacing and time discretization. The mesh has been refined using 4 levels on the h-refinement criteria with a ratio of 1.5 (i.e. in each computational level, denoted with letter 'm' the mesh is increased 1.5 times, see Table 1). Table 1 shows also the control volume distribution for each element of the physical domain, i.e. air, solid walls, insulation material and water. To perform the verification of the numerical solution, the problem has been solved up to 7200 s. Moreover, for each instant, three characteristic values have been calculated: i) the mean water temperature; ii) the mean internal wall temperature; iii) the average Nusselt number. The previous characteristics have been calculated as follows: the mean fluid temperature:

$$\bar{T}_f = \frac{1}{\Omega} \int_{\Omega} T d\Omega \quad (4)$$

the mean wall temperature:

$$\bar{T}_w = \frac{1}{S} \int_S T dS \quad (5)$$

the average Nusselt number at the internal walls:

$$\overline{Nu} = \frac{1}{(\bar{T} - \bar{T}_w)S} \int_S \left(\frac{\partial T}{\partial n} \right) dS \quad (6)$$

In order to point out the differences between the variety of used grids, the computational error has been estimated. Numerical solutions for each computational grid have been compared with the finest mesh solution taken as the most accurate solution. For each solution in the h-refinement, the relative error ε has been estimated. As the finest mesh solution is used as reference solution, its relative error is equal to 0 (indicated with a dash). Tables 2–4 summarize the post-processing results. For the water and wall temperatures, the errors found by the different mesh levels are lower than 0.2%. For the Nusselt number, as the mesh is refined, the discrepancies are reduced. An error less than 3% has been obtained using the third mesh level. Moreover, as time goes by, these discrepancies tend to level out.

To reduce the computational time and computer memory requirements while providing accurate results, the mesh selected should be a compromise between both criteria. Thus, as the results for the third (m_3) and the finest level (m_4) of refinement are almost identical, the third level of refinement mesh has been used in CFD results presented in further sections.

In addition to mesh verification, temporal discretization has been also verified by using time steps of 0.01 s, 0.1 s, 0.5 s, 1 s. As the

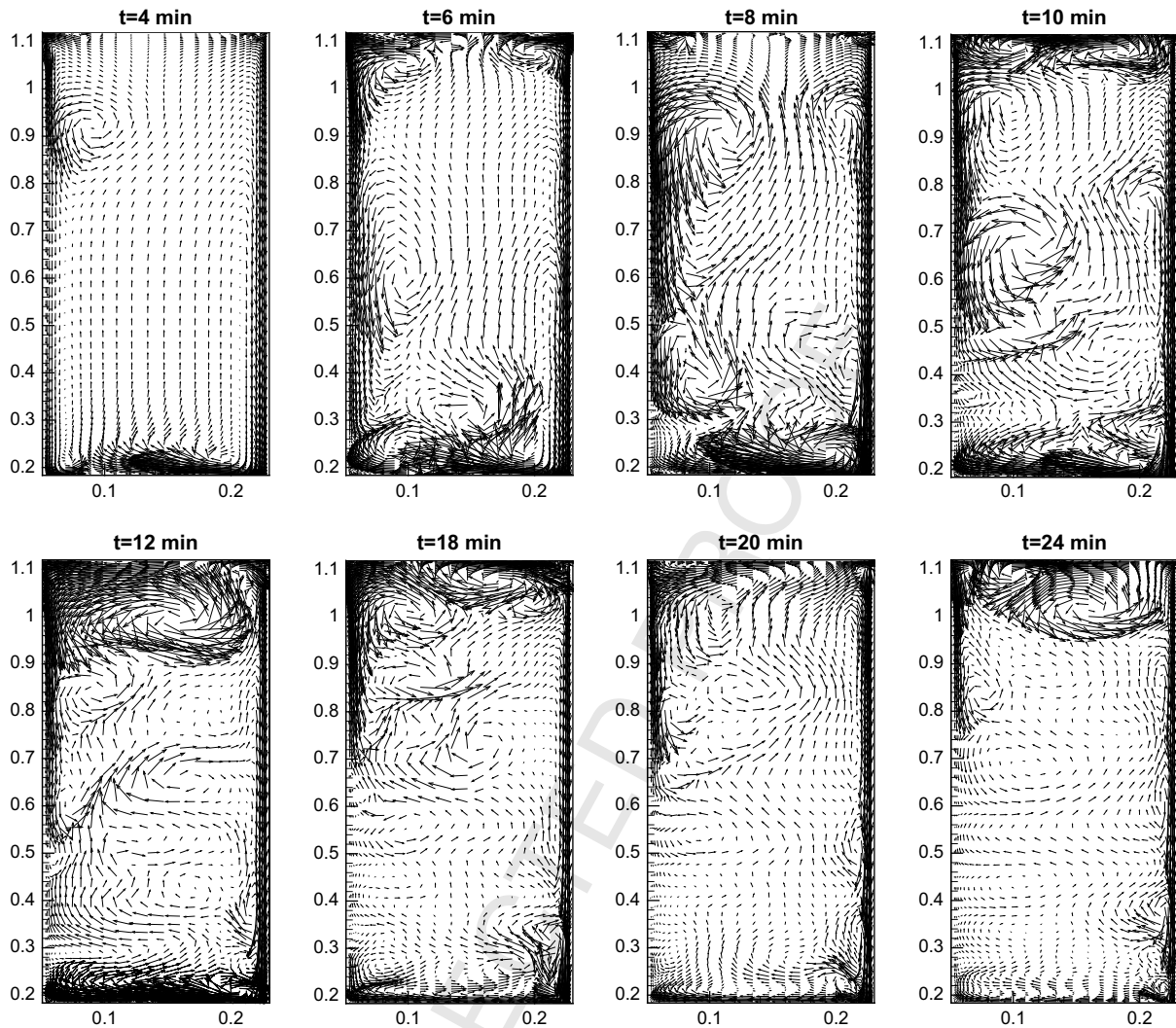


Fig. 7. Transient evolution of the fluid inside the water store. Velocity vectors during cooling process for time = 4–24 min.

computational domain includes two different fluids (water, air) and two different materials (steel, polyurethane), it has been difficult to optimise the time step to be used. For time step of 1 s, the convergence has been unstable and in most time steps the convergence criteria has not been satisfied after 400 iterations. For time step of $\Delta t = 0.5$ s, convergence has been reached after more than 100 iterations. Furthermore, after 1000 s, the convergence became unstable. For the two smallest time increments, the number of iterations has been always below 50 even for the first instants, and around 5 and 1 for $\Delta t = 0.1$ s and $\Delta t = 0.01$ s respectively for the most time of the cooling process. No significant differences have been observed among the results obtained with the smallest time steps. However, CPU time has been very high for the time increment of 0.01 s. Therefore, as the time to cool-down the tank is very large, it has been decided to simulate the case with a time step of $\Delta t = 0.1$ s.

4.2. Validation of the numerical results

As have been commented before, the long-term cooling process of the tank with homogeneous initial temperature of 65°C has been studied numerically and experimentally. Thus a long-term cooling test with an initial conditions of uniform temperature of 65°C has been carried out. The comparison between experimental

and numerical data for the water inside the tank is shown in Fig. 3. In the latter figure, the temperature profile at different tank heights are represented. This figure shows that, even after 90 h of the cooling process, the numerical simulation is able to reproduce the experimental data with a good accuracy. At the tank bottom, it can be observed a marked increase of the thermal gradient in the vertical direction. During the cooling process, stratification progresses from the bottom of the tank to its top. This is due to heat losses from the stored fluid to the ambient and the gas flue. The fluid temperature drop near the vertical tank wall forms a boundary layer with a descending fluid and thus, due to buoyancy effects, bottom layers are filled with cold fluid, resulting in the development of a temperature gradient inside the storage tank. The same behaviour was observed in the study of Oliveski et al. [12]. However, for the present case the thermal gradient is more noticeable due to the heat losses to the combustion chamber through the bottom wall of the storage tank. A detailed comparison of temperature profile between calculation and measurement as a function of time at different tank height locations is presented in Fig. 4. It can be observed that there is a good agreement between numerical and experimental results for the 90 h of the cooling process and for the different thermal water layers.

Regarding the air in the chimney, the comparison between the numerical and experimental results are given in Fig. 5. By analysing

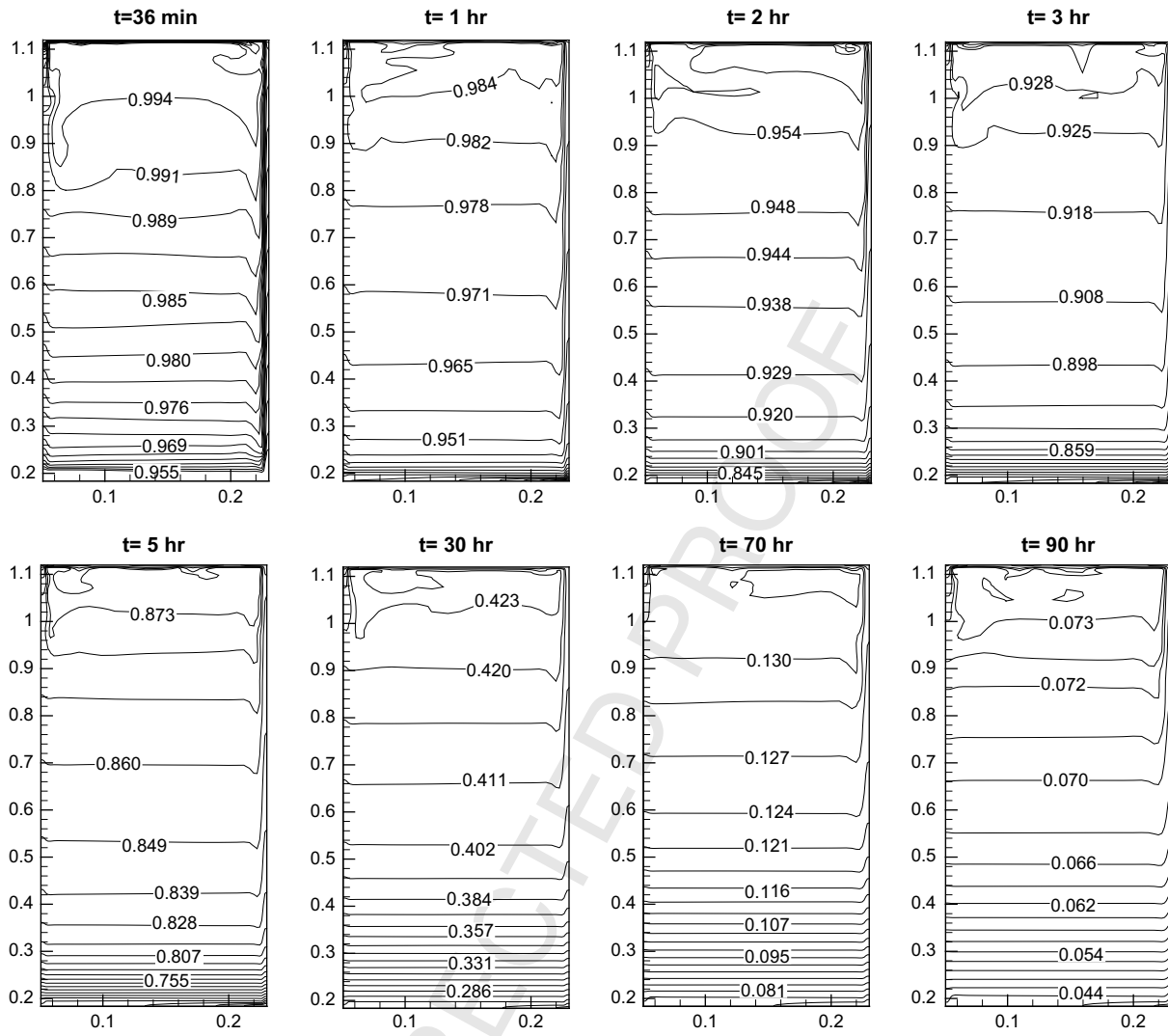


Fig. 8. Transient evolution of the fluid inside the water store. Dimensionless temperature contour during cooling process for time = 36 min to time = 90 h.

the figure, it can be seen that, during the 90 h of the cooling process, the numerical results show the same tendency as the experimental data. Moreover, for the different heights of the gas flue, a good agreement between the numerical and the experimental results has been obtained. Thus, the heat exchanges between the water and the air inside the gas flue have been well simulated. However, inside the combustion chamber (see Fig. 5 (e)), the numerical solution shows some discrepancies due to inconsistency in the estimation of the real rate of entering air and the use of the axisymmetric approximation. Indeed, it is observed in Fig. 5 (e) that the numerical model over predicts the air temperature. This is mainly due to the under estimated air mass flow rate imposed as inlet boundary condition in the numerical model.

It is also observed that, for the different gas flue heights, unsteady temperature profile has been obtained which is in disagreement with other models described in the literature; those models assume a constant temperature along the gas flue and during the cooling process [16].

In general, the temperature profiles are comparable but minor discrepancies between experiments and calculation have been observed especially in the lower part of the tank. Those differences can be due to different factors such as: i) the inconsistency between the experimental rate of air entering the chimney and that imposed in the CFD simulation; ii) the insulation layer is not uniformly

distributed in the experimental prototype, which can introduce some discrepancies with the constant insulation thickness modelled by the CFD code; iii) another source of discrepancies is the axisymmetric approximation used in the developed code; iv) the thermo-physical properties of the real materials are not known thus, in the model these properties have been taken from the literature and v) the fixed initial constant temperature through the gas flue in the numerical calculations.

5. Transient flow patterns

To provide a comprehensive and direct perception of the transient evolving process of natural convection flow in the water store, time evolution of temperature profiles and velocity vectors in the water part of the domain are presented in Figs. 6–9. In these figures, the fluid temperature has been plotted using the non-dimensional variable:

$$\theta = \frac{T - T_{\text{amb}}}{T_{\text{ini}} - T_{\text{amb}}} \quad (7)$$

It is seen that, when the sidewall is cooled due to heat losses to the environment and the internal wall is cooled due to the heat exchange with the cold air inside the chimney, two vertical thermal

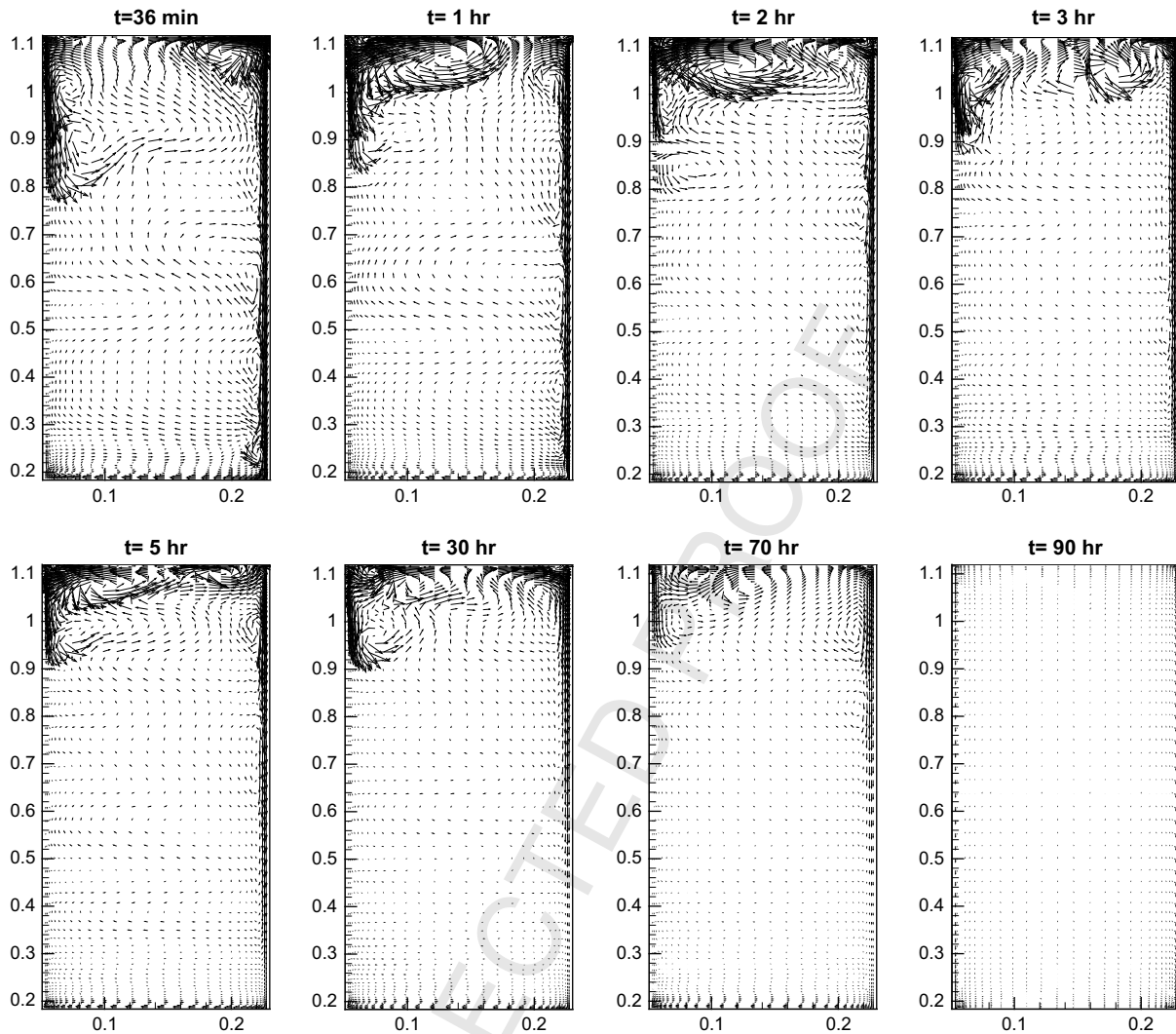


Fig. 9. Transient evolution of the fluid inside the water store. Velocity vectors during cooling process for time = 36 min to time = 90 h.

boundary layers develop very rapidly on the two walls (see $t = 4$ min Figs. 6 and 7). After the full development of the vertical thermal boundary layers, a cold intrusion begins to form and moves continuously along the bottom wall towards the inside wall. As the intrusion approaches the inside wall, the wave increases in size and its shape changes gradually due to the interaction between the intrusion and the cooled fluid near to the chimney wall. Thus, crests in the temperature fields are formed (see $t = 6$ min in Fig. 6). As in the bottom wall there is an interaction between the two cooled fluids travelling down, in the sidewall and in the chimney wall, waves move back and forth at the bottom (see $t = 8$ – 10 min in Figs. 6 and 7). When moving up, the fluid interacts continuously with the cooled fluid flowing down along the two vertical walls, thus create a crests in the core of the tank. This phenomena is well illustrated in Fig. 7, where velocity vectors are shown.

As results of this movement, there is a mixing between the cold travelling stream and the surrounding fluid at the bottom, forming layers of fluid at different temperatures. Thus, the temperature of the intruding cold fluid at the bottom increases until its motion vanishes (see $t = 12$ – 24 min in Figs. 6 and 7). Meanwhile, thermal stratified layers have been generated inside the tank.

As thermal stratification gradually advances from bottom to top, interactions between cooled fluid in the two vertical sidewalls and

the fluid in the core of the tank are more concentrated in the upper part. This is mainly due to the presence of the temperature gradient in the bottom region where diffusion heat transfer mechanism dominates. Similar fluid behaviour has been described previously in the literature [11,15]. However, these studies did not consider the presence of a gas flue inside the tank.

In Figs. 8 and 9 (from $t = 36$ min to $t = 2$ h), it is shown how the stratification in the bottom zone is completely developed and how vortices are displaced from the centre to the top. Due to the chimney effect in the gas flue (the hot air tends to be in the top while the cold is in the bottom), the heat transfer at the top region near to the chimney wall is more intense promoting the mixing of the fluid around that zones and, as a consequence, the increasing of the heat losses to the environment.

Indeed, by analysing the fluid structure inside the tank after 3 h of the cooling process, it is shown that the flow structure can be divided in two regions; convective effects near to the top wall and the left corner of the chimney wall, and diffusive effects in the bottom part of the tank (see $t = 3$ – 30 h in Figs. 8 and 9). During that period a quasi-steady regime starts to be reached. As time progresses, the unsteady natural convection flow and the generation of the thermal stratification are progressively reduced until reaching a quasi-steady regime and consequently a very slow movement of

the fluid is observed. This process continues until the cooling process ends (see $t = 70\text{--}90$ h in Figs. 8 and 9).

6. Conclusion

In the present work the cooling process by laminar natural convection of a vertical cylindrical tank with an internal gas flue has been analysed numerically and experimentally. The fluids (water and air) have been considered at a constant initial temperature. The computational domain has been extended up to an external thin layer of steel, taking also into account the internal solid wall and the insulation material.

The obtained numerical solutions have been verified by analysing the results of four levels of refinement in the spatial domain. In the verification process, the results of each level have been compared to those of the finest grid. On the other hand, the influence of the time discretization has also been considered, by analysing four time increments. Considering both, the results of the spatial and temporal discretization and the long period to be simulated, the third level of grid refinement with a time step of 0.1 s have been chosen.

An experimental test of the long-term cooling process has been carried out in order to validate the developed numerical model. For a period of 90 h, a good agreement between experimental data and numerical results has been observed. Therefore, taking into account the independence of the adopted grids, it is concluded that the developed model can be used to simulate similar situations and geometries with reliable results.

The detailed analysis of the cooling process has also been shown. By analysing the numerical solution, it has been observed that in the first hours of the cooling process, when the fluid is stratified from the bottom to the top of the tank a quasi-steady regime is reached. At this regime, the flow can be divided in two regions; i.e. convective effects in the superior half and diffusive effects in the inferior half of the tank. The predominance of the diffusive effects in the bottom zone provides a thermal stratification of the fluid.

It has been shown that the numerical model is able to describe in detail the phenomena that occur inside the storage tank with an internal gas flue during the whole cooling process with a better prediction of the thermal and hydrodynamic behaviour of the study case. It is important to point out, that the results obtained from this kind of numerical simulation can be used not only for the assessment of innovative designs, but also in the development of correlations with the objective to feed simplified models.

References

- [1] TRNSYS group, A Transient System Simulation Program TRNSYS, Solar Energy Laboratory, University of Wisconsin, Madison, 1994.
- [2] E.M. Kleinbach, W.A. Beckman, S.A. Klein, Performance study of one-dimensional models for stratified thermal storage tanks, *Solar Energy* 50 (2) (1993) 155–166.
- [3] J.A. Duffie, W.A. Beckman, *Solar Engineering of Thermal Processes*, second ed. Wiley Inter Science, New York, 1991.
- [4] Y.H. Zurigat, A.J. Ghajar, P.M. Moretti, Comparison study of one-dimensional models for stratified thermal storage tanks, *Applied Energy* 30 (1988) 99–111.
- [5] S. Alizadeh, An experimental and numerical study of thermal stratification in a horizontal cylindrical solar storage tank, *Solar Energy* 66 (6) (1999) 409–421.
- [6] J.M. Hyun, Transient process of thermally stratifying an initially homogeneous fluid in an enclosure, *International Journal of Heat and Mass Transfer* 27 (10) (1984) 1936–1938.
- [7] M. Cotter, M. Charles, Transient cooling of petroleum by natural convection in cylindrical storage tanks. I. Development and testing the numerical simulator, *International Journal of Heat and Mass Transfer* 36 (8) (1993) 2165–2174.
- [8] M. Cotter, M. Charles, Transient cooling of petroleum by natural convection in cylindrical storage tanks. II. Effect of heat transfer coefficient, aspect ratio and temperature-dependent viscosity, *International Journal of Heat and Mass Transfer* 36 (8) (1993) 2175–2182.
- [9] E. Papanicolaou, V. Belessiotis, Transient natural convection in a cylindrical enclosure at high Rayleigh numbers, *International Journal of Heat and Mass Transfer* 45 (7) (2002) 1425–1444.
- [10] W. Lin, S.W. Armfield, Direct simulation of natural convection cooling in a vertical circular cylinder, *International Journal of Heat and Mass Transfer* 42 (22) (1999) 4117–4130.
- [11] W. Lin, S.W. Armfield, Long-term behaviour of cooling fluid in a vertical cylinder, *International Journal of Heat and Mass Transfer* 48 (1) (2005) 53–66.
- [12] R.C. Oliveski, A. Krenzinger, H.A. Vielmo, Cooling of cylindrical tanks submitted to natural internal convection, *International Journal of Heat and Mass Transfer* 46 (2003) 2015–2026.
- [13] R.C. Oliveski, A. Krenzinger, H.A. Vielmo, Comparison between models for the simulation of hot water storage tanks, *Solar Energy* 75 (2) (2003) 121–134.
- [14] J. Fernandez-Seara, J. Uria Francisco, J. Sieres, Experimental analysis of a domestic electric hot water storage tank. Part I: static mode of operation, *Applied Thermal Engineering* 27 (1) (2007) 129–136.
- [15] I. Rodriguez, J. Castro, C.D. Pérez-Segarra, A. Oliva, Unsteady numerical simulation of the cooling process of vertical storage tanks under laminar natural convection, *International Journal of Thermal Sciences* 48 (4) (2009) 708–721.
- [16] J. Newton, Modelling of Solar Storage Tanks, Master of Science Mechanical Engineering, University of Wisconsin, Madison, 1995.
- [17] I. Hmouda, C. Bouden, Modélisation du Comportement d'un Accumulateur avec Brûleur à Gaz Intégré, in: *The International Congress on the Renewable Energies and the Environment CER 2005*, Sousse, Tunisia, 2005.
- [18] I. Hmouda, C. Bouden, A new TRNSYS model for stratified fluid storage tanks with an integrated gas heater, in: *Solar World Congress ISES 2005*, Orlando, Florida, USA, 2005.
- [19] I. Hmouda, C. Bouden, Etude Paramétrique d'un Chauffe-eau Solaire Avec Appoint à Gaz Intégré Dans le Ballon de Stockage en vue de l'optimisation de la Position du Brûleur, 12èmes Journées Internationales de Thermique JITH2005, Tanger Morocco, 2005.
- [20] X. Trias, M. Soria, C.D. Pérez-Segarra, A. Oliva, Direct numerical simulations of two and three dimensional turbulent natural convection flows in a differentially heated cavity of aspect ratio 4, *Journal of Fluid Mechanics* 586 (2007) 259–293.
- [21] C.F. Hess, C.W. Miller, Natural convection in a vertical cylinder subject to constant heat flux, *International Journal of Heat and Mass Transfer* 22 (1979) 421–430.
- [22] I. Hmouda, C. Bouden, Parameters identification of a water storage tank fired by a gas heater and modelling of its thermal behaviour, in: *The Second International Conference on Advances Mechanical Engineering ICAME 2004*, The Tunisian Scientific Society, Tunisia, 2004.
- [23] S.V. Patankar, *Numerical Heat Transfer and Fluid Flow*, McGraw-Hill, New York, 1980.
- [24] P.H. Gaskell, A.K.C. Lau, Curvature-compensated convective transport: SMART, a new boundedness-preserving transport algorithm, *International Journal for Numerical Methods in Fluids* 8 (1988) 617–641.
- [25] J.P. Van Doormaal, G.D. Raithby, Enhancements of the SIMPLE method for predicting incompressible fluid flow, *Numerical Heat Transfer* 7 (1984) 147–163.
- [26] W.H. Press, et al., *Numerical Recipes in C. The Art of Scientific Computing*, Cambridge University Press, 1994.
- [27] C.D. Pérez-Segarra, A. Oliva, M. Costa, F. Escanes, Numerical experiments in turbulent natural and mixed convection in internal flows, *International Journal for Numerical Methods for Heat and Fluid Flow* 5 (1) (1995) 13–33.